# NJC

Accepted Manuscript


This is an *Accepted Manuscript*, which has been through the Royal Society of Chemistry peer review process and has been accepted for publication.

*Accepted Manuscripts* are published online shortly after acceptance, before technical editing, formatting and proof reading. Using this free service, authors can make their results available to the community, in citable form, before we publish the edited article. We will replace this *Accepted Manuscript* with the edited and formatted *Advance Article* as soon as it is available.

You can find more information about *Accepted Manuscripts* in the Information for Authors.

Please note that technical editing may introduce minor changes to the text and/or graphics, which may alter content. The journal's standard Terms & Conditions and the Ethical guidelines still apply. In no event shall the Royal Society of Chemistry be held responsible for any errors or omissions in this *Accepted Manuscript* or any consequences arising from the use of any information it contains.

ROYAL SOCIETY OF CHEMISTRY

www.rsc.org/njc

# Reactivity of silica supported zirconium hydride with $N_2O$ and $CO_2$ probe molecules: a computational point of view.

**Mahboubeh Poor Kalhor,[a] Raphael Wischert,[b†1] Christophe Copéret,[b,*] Henry Chermette,[a,*]**

[a] University of Lyon; Université Lyon 1(UCBL) and UMR CNRS 5280 Institut Sciences Analytiques, F-69622 Villeurbanne Cedex, France

[b] Department of Chemistry and Applied Biosciences, ETH Zürich, Vladimir Prelog Weg 2, CH-8093 Zürich, Switzerland.

## Abstract

The reactivity of supported zirconium hydrides toward probe molecules like $N_2O$ and $CO_2$ have shown that both hydrides are converted to the corresponding hydroxide and formate species, which were characterized by IR and NMR spectroscopies. Their reactivity towards these probe molecules is analyzed through DFT (Density Functional Theory) calculations. The computed spectroscopic IR and NMR signatures are fully consistent with experimental observations.



[1] †Present address: Eco-Efficient Products and Processes Laboratory (E2P2L), UMI 3464 CNRS – Solvay, 3966 Jin Du Road, Xin Zhuang Ind. Zone, 201108 Shanghai, China.

## Introduction

Supported early transition-metal hydrides present unprecedented reactivities by comparison to many of their molecular analogues.[1-3] Besides the hydrogenation of olefins and aromatics, zirconium hydrides, discovered in the late seventies[4] readily activate the C-H bond of alkanes[5] and more importantly catalyze the hydrogenolysis of alkanes[6], including polyethylene[7] and even the homologation of alkanes in the absence of hydrogen.[8] Advanced spectroscopic studies have shown that the silica-supported zirconium hydrides, prepared via the hydrogenolysis of the well-defined zirconium trisneopentyl siloxy complex, present two main surface species, a mono- and a bis-hydride, which display distinct spectroscopic signatures (both in IR and in NMR) and reactivities.[9, 10] In particular, the investigation of the reactivity of supported zirconium hydrides toward probe molecules like $N_2O$ and $CO_2$ has shown that both hydrides are converted to the corresponding hydroxide and formate species, which were characterized by IR and NMR spectroscopies. In addition, the reaction with $CO_2$ yielded small amounts of methoxide surface species. Such methoxide was proposed to originate from the reaction of the dihydride with $CO_2$ to yield a dioxazirconacyclobutane; its decomposition into formaldehyde and the subsequent reaction of the latter with another metal hydride yielding the methoxide. Following our investigation of the reactivity of these hydrides towards alkanes, where we showed that σ-bond metathesis was a key step in the C-H bond activation of alkanes[11], we have here explored their reactivity towards $N_2O$ and $CO_2$ probe molecules through DFT (Density Functional Theory) calculations.

## Computational details

The Amsterdam Density Functional (ADF) code was herein used [12-14] in combination with PW91 gradient-corrected exchange–correlation functional [15-17] and the Triple Zeta plus Polarisation (TZP) basis. All the structures were characterized by vibrational analysis in the

harmonic approximation with no imaginary frequency for stable states (energy minima) and one imaginary frequency for transition states. Similar computation parameters have proved to be adequate for the study of analogous systems[11,18-20]. Charges were condensed on atoms following Mulliken scheme.

## Modelling metal hydrides.

The zirconium monohydride $(SiO)_3ZrH$ and dihydride $(SiO)_2ZrH_2$ surface sites were modelled using clusters of three (**1-H**) and two silicon atoms (**2-H**), respectively (Figure 1), where the dangling bond were replaced by OH groups.[10, 11, 21-23] The calculated average distances between the surface oxygen and zirconium in **1-H** and **2-H** (1.98 Å and 1.96 Å, respectively) are close to those determined experimentally by EXAFS (1.95 Å).[11] Furthermore, the calculated frequencies of vibration of Zr-H in **1-H** is 1602 $cm^{-1}$ and in **2-H** are 1610 $cm^{-1}$ and 1634 $cm^{-1}$, which are very close to the experimental value observed in IR spectroscopy (a broad complex band at 1638 $cm^{-1}$,[9]) which has been attributed to the mono- and the bis-hydride.[10] In addition, the calculated proton NMR chemical shifts, considering spin orbit corrections,[24] for **1-H** and **2-H** are 10.3 and 10.9 ppm, respectively in close agreement with experiments, where the corresponding species have distinct chemical shifts of 10.1 and 12.0 ppm, respectively.[9] Overall, calculated data is in close agreement with experiment, indicating with good confidence that the cluster model represents quite well the actual surface sites present in the silica-supported zirconium hydrides.[25]

*--- insert Fig. 1 near here ---*

## Reactivity of zirconium hydrides with $N_2O$

The reaction of **1-H** with $N_2O$ giving the corresponding monohydroxide **1-OH** is strongly exothermic, $\Delta E_0$ = –345 kJ.mol$^{-1}$, which is consistent with the simultaneous formation of a strong Zr-O bond and the very stable dinitrogen molecule. This reaction is associated with a small energy barrier of ca. 53.6 kJ.mol$^{-1}$, consistent with the observed reactivity at room temperature. In addition, the calculated frequencies of vibration of ZrO-H in **1-OH** is 3786 cm$^{-1}$ – red shifted by 20 cm$^{-1}$ with respect to SiO-H (3766 cm$^{-1}$) – in excellent agreement with the experimental values (3785 cm$^{-1}$ vs. 3747 cm$^{-1}$).[9] Finally, the NMR calculations show a signal at 4.66 ppm for **1-OH** which is also close to the experimental value (4.1 ppm).[9]

*--- insert Fig. 2 here ---*

The corresponding transition-state (**TS1**) describes the direct insertion of O into the Zr-H bond, accompanied by the loss of $N_2$ (Figure 2). The elongation of Zr-H, N-O and N-N bond distances, 0.085 Å, 0.23 Å and 0.84 Å, respectively, in the **TS1**, compared with **1-H** and $N_2O$ shows the weakening of these bonds to produce **1-OH** and $N_2$. Note the increase of the positive (Mulliken) charge at Zr (+0.09) and of the negative charge at the oxygen atom of $N_2O$ (–0.12), and the decrease of the negative charge of the hydrogen atoms connected to Zr and positive charge of nitrogen connected to oxygen of $N_2O$ (+0.10 and -0.15, respectively), which suggests a charge transfer from the HOMO of **1** (Hydrogen 1s and complex d) toward the LUMO of $N_2O$ ($p_x$) (Figure S2), in other words an electrophilic activation of $N_2O$. In line with this, the (mostly) interacting orbitals are the HOMO of **1-H** and the LUMO of $N_2O$ (see Figure 3).

*--- insert Fig. 3 here ---*

The fact that $N_2O$ can also coordinate in an O-bound fashion (whereas the HOMO of $N_2O$ is mostly centered on nitrogen) is undoubtedly related to the charge interaction between the (almost 2+) positive charge of the zirconium and the most negative charged atom of $N_2O$, namely oxygen. This is in agreement with the large hardness of the reactants (as measured by the HOMO-LUMO gap) which favors the charged controlled reactions. Note that the N-bound $N_2O$ is only slightly exothermic, ($\Delta E_0$ = –6 kJ.mol$^{-1}$) with a linear Zr-N-N-O structure; however it was not possible to locate a reactive pathway.

For the dihydride **2-H**, it has been possible to localize the intermediate (**2-H•$N_2O$**), which corresponds to the coordination of $N_2O$ on zirconium; it is -19 kJ.mol$^{-1}$ more stable than the separated reactants, where the oxygen of $N_2O$ is coordinated to now a bipyramidal Zr complex thus inducing a lengthening of the N-O distance by 0.77 Å. From this intermediate, the first and the second insertion processes leading to a monohydroxy, **2-(H)(OH)**, and the bis-hydroxy **2-$(OH)_2$** complexes are each exoenergetic by -354 and -335 kJ.mol$^{-1}$ respectively (Figures 4 and S3), values very close to this found for the reaction of **1-H** and $N_2O$ (-345.2 kJ.mol$^{-1}$), making overall the formation of the dihydroxide highly exoenergetic (-689 kJ.mol$^{-1}$). Here again, one may point out the existence of a N-bound fashion coordination leading to a slightly exothermic, ($\Delta E_0$ = –26 kJ.mol$^{-1}$) formation of a stable intermediate adduct with a linear Zr-N-N-O structure, and again it was not possible to locate a reactive pathway."

*--- insert Fig. 4 here ---*

These steps are associated with low energy TS (**TS2** and **TS3**) states (71.5 kJ.mol$^{-1}$ and 62.5 kJ.mol$^{-1}$), again compatible with the easy conversion of the bis-hydride to the bis-hydroxide at room temperature as observed experimentally. Note that the elimination of water from **2-$(OH)_2$** to form the oxide **2-(Oxo)** is clearly disfavoured as evidenced by the highly endoenergetic process ($\Delta E_0$= 252.9 kJ/mol and $\Delta G°$=213.6 kJ/mol). The calculated IR and NMR signatures are also in good agreement with experiment: vibration frequencies of ZrO-H

in **2-(OH)$_2$** are 3770 cm$^{-1}$ and 3781 cm$^{-1}$ (red shifted by 14.5 cm$^{-1}$ and 25.5 cm$^{-1}$ with respect to SiO-H (3755.5 cm$^{-1}$), respectively and the calculated chemical shift of 5.08 ppm and 5.84 ppm for **2-(OH)$_2$**. Note that the calculated vibration frequencies of ZrO-H, Zr-H and SiO-H in **2-(H)(OH)** are 3781 cm$^{-1}$, 1625 cm$^{-1}$ and 3756 cm$^{-1}$, respectively and that the corresponding chemical shifts are 5.18 (ZrO-H) and 9.51 (Zr-H) ppm for **2-(H)(OH)**, which are not observed experimentally in line with the high reactivity of that intermediate.

The first insertion step is associated with a transition state, where $N_2O$ is found in between the two hydride ligands, with one of the hydride very close to the O atoms (1.739 vs. 2.652 Å). The second step involves a transition state very similar to the one described in the reaction of **1-H** with $N_2O$, with a TBP geometry. As in the case of the reaction between $(SiO)_3ZrH$ and $N_2O$, a similar change of charges on the Zr, H, O, N atoms and of ΔE between HOMOs and LUMOs of **2-H** and $N_2O$ is obtained, corresponding to a charge transfer from the HOMO of **2-H** toward the LUMO of $N_2O$ (Figures S4 and S5): increase of the positive charge of Zr and the negative charge of oxygen atom of $N_2O$ (+0.09 and -0.07, respectively) and a decrease of the negative charge of the hydrogen atoms connected to Zr and of the positive charge of nitrogen connected to oxygen of $N_2O$ (+0.16 and -0.21, respectively). All data converge to describe a charge transfer from the HOMO of **2-(H)(OH)** towards the LUMO of $N_2O$ (Figure S4 and Figure S6).

## Reactivity of zirconium hydrides with $CO_2$:

The reaction of **1-H** and $CO_2$ leads to the formation of a weak $CO_2$-adduct (**1-H•CO$_2$**) with a stabilization energy of -15.6 kJ.mol$^{-1}$, which yields $\eta^1$– then a $\eta^2$–formate species, noted (**1-$\eta^1$-O$_2$CH**) and (**1-$\eta^2$-O$_2$CH**) respectively, with high reaction energies of –135 and -183 kJ.mol$^{-1}$, with respect to separated reactants (**1-H** and $CO_2$). The formation of **1-$\eta^1$-O$_2$CH** and **1-$\eta^2$-O$_2$CH** is practically barrierless, with very low activation energies of 1.1 kJ.mol$^{-1}$ and 0.6 kJ.mol$^{-1}$, respectively. The calculated vibrational frequency of the C-H bond in **1-$\eta^2$-O$_2$CH**

(2996 $cm^{-1}$) is in agreement with experiment (2960 $cm^{-1}$).[9] In addition, the calculated proton and carbon-13 chemical shifts for **1-η²-O₂CH** are 9.4 ppm and 187 ppm, in close agreement with experiment (8.7 ppm and 183 ppm, respectively).

*--- insert Fig. 5 here ---*

In the **TS4**, the approach of $CO_2$ to Zr-H bond is evidenced by the shortening of the distances between C---H and Zr---O($CO_2$), with respect to **1-H•CO₂** by 0.49 Å and 0.11 Å, respectively, leading to the formation of the O-Zr bond in **1-η¹-O₂CH**. This step is associated with a very low activation energy (1.1 $kJ.mol^{-1}$), and subsequently **1-η¹-O₂CH** yields the more stable $\eta^2$-compound **1-η²-O₂CH**, which is again an essentially barrierless process (0.4 $kJ.mol^{-1}$, Figure 6 and S7).

*--- insert Fig. 6 here ---*

A comparison of the Mulliken charges in **1-H•CO₂** and the transition state shows an increase in the positive charge of Zr and the negative charge of oxygen of $CO_2$ (+0.04 and -0.03, respectively) and a decrease of the negative charge of H of the complex and a positive charge of C (+0.10 and -0.04, respectively) (Figure S8). These results, coupled to the small ΔE between HOMOs and LUMOs, are consistent with a charge transfer from the HOMO of the complex to the LUMO of $CO_2$ (Figure S9).

For the dihydride **2-H**, a weak $CO_2$ adduct (**2-H•CO₂**) is also located; it is -17.7 $kJ.mol^{-1}$ more stable than separated reactants (**2-H + CO₂**). Similarly to $N_2O$, $CO_2$ coordinates to zirconium between the two hydride ligands through one of its oxygen atoms. From this intermediate, insertion of $CO_2$ leads first to the formation of $\eta^1$– and then $\eta^2$–mono–formate species, noted **2-(H)(η¹-O₂CH)** and **2-(H)(η²-O₂CH)**, and then to the corresponding $\eta^1$– and $\eta^2$–bis–formate species **2-(η¹-O₂CH)₂** and **2–(η²-O₂CH)₂** via processes similar to what was discussed for **1-H**. All these processes are highly exoenergetic (Figures 6a and 6b). The $CO_2$

insertion steps from **2-H** or **2-(H)($\eta^2$-$O_2$CH)** leading to the $\eta^1$–formates are both essentially barrierless (< 1 kJ.mol$^{-1}$), while the change of coordination of the formate ligand from $\eta^1$ to $\eta^2$ is associated with slightly higher energy barriers (ca. 27-28 kJ.mol$^{-1}$ for the first step, and barrierless for the second step) (Figures 6a and b and S10-13). This energy schemes are consistent with a very facile process. The calculated vibrational frequency of the C-H bond in **2-(H)($\eta^2$-$O_2$CH)** is 2978 cm$^{-1}$, while the calculated protons and carbon-13 chemical shifts for **2-(H)($\eta^2$-$O_2$CH)** are 10.6 (Zr-*H*), 9.8 ppm (Zr-($\eta^2$-$O_2$C-*H*)) and 191.3 ppm (Zr-($\eta^2$-$O_2$*C*-H)), respectively. The presence of such hydrides has not been observed experimentally, but the computed spectroscopic signatures for 2–($\eta^2$-$O_2$CH)$_2$ (2996 and 2999 cm$^{-1}$ for the C-H bond vibration and $\delta_H$= 9.4 ppm and $\delta$□□=185.7 ppm) are fully consistent with experimental values. In the case of **2-H**, the intramolecular insertion of the remaining hydride into the adjacent formate has also been examined. While this step is slightly exoenergetic, it is associated with an energy barrier of 125.6 kJ.mol$^{-1}$ (See Figure S14), indicating that this reaction is difficult, not to say unlikely at room temperature. From this intermediate, we also examine further decomposition step, such as the formation of 2-(O) and formaldehyde, but this step has been found to be highly endoenergetic ($\Delta E_0$= 191.3 kJ.mol$^{-1}$ and $\Delta G^0$ = 146.8 kJ.mol$^{-1}$), which is very unfavorable and probably associated with a high energy barrier (it was not possible to locate a TS).

## Conclusion

This computational study shows that silica-supported zirconium mono- and bis-hydride surface species have very similar spectroscopic NMR and IR signatures as well as reactivity towards $N_2O$ and $CO_2$, leading to the corresponding hydroxide and formate derivatives. These species display computed spectroscopic IR and NMR signatures, fully consistent with observation, further supporting prior proposition. Note however that no reaction pathway

leading to the formation of methoxy surface species upon reaction of $CO_2$ and zirconium hydrides could be located, pointing out to the possibility of additional minor species, such as a putative trishydride.

## Acknowledgments:

The authors gratefully acknowledge the GENCI/CINES for HPC resources/computer time (Project cpt2130). They warmly thank Thomas Gianetti for preliminary calculations and discussions.

## References:


1. C. Thieuleux, C. Coperet, V. Dufaud, C. Marangelli, E. Kuntz and J. M. Basset, *Journal of Molecular Catalysis a-Chemical*, 2004, **213**, 47-57.
2. C. Coperet, *Chemical Reviews*, **110**, 656-680.
3. J. M. Basset, C. Coperet, D. Soulivong, M. Taoufik and J. T. Cazat, *Accounts of Chemical Research*, **43**, 323-334.
4. Y. I. Yermakov, Y. A. Ryndin, O. S. Alekseev, D. I. Kochubey, V. A. Shmachkov and N. I. Gergert, *Journal of Molecular Catalysis*, 1989, **49**, 121-132.
5. F. Quignard, C. Lecuyer, C. Bougault, F. Lefebvre, A. Choplin, D. Olivier and J. M. Basset, *Inorganic Chemistry*, 1992, **31**, 928-930.
6. C. Lecuyer, F. Quignard, A. Choplin, D. Olivier and J. M. Basset, *Angewandte Chemie-International Edition in English*, 1991, **30**, 1660-1661.
7. V. R. Dufaud and J. M. Basset, *Angewandte Chemie-International Edition*, 1998, **37**, 806-810.
8. C. Thieuleux, A. Maraval, L. Veyre, C. Coperet, D. Soulivong, J. M. Basset and G. J. Sunley, *Angewandte Chemie-International Edition*, 2007, **46**, 2288-2290.
9. F. Rataboul, A. Baudouin, C. Thieuleux, L. Veyre, C. Coperet, J. Thivolle-Cazat, J. M. Basset, A. Lesage and L. Emsley, *Journal of the American Chemical Society*, 2004, **126**, 12541-12550.
10. C. Thieuleux, E. A. Quadrelli, J. M. Basset, J. Dobler and J. Sauer, *Chemical Communications*, 2004, 1729-1731.
11. C. Coperet, A. Grouiller, J. M. Basset and H. Chermette, *Chemphyschem*, 2003, **4**, 608-611.
12. G. te Velde, F. M. Bickelhaupt, S. J. A. van Gisbergen, C. Fonseca Guerra, E. J. Baerends, J. G. Snijders and T. Ziegler, *J. Comput. Chem.*, 2001, **22**, 931.
13. C. Fonseca Guerra, J. G. Snijders, G. te Velde and E. J. Baerends, *Theor. Chem. Acc.*, 1998, **99**, 391.
14. J. A. E.J. Baerends, A. Bérces, F.M. Bickelhaupt, C. Bo, P.M. Boerrigter, L. Cavallo, D.P. Chong, L. Deng, R.M. Dickson, D.E. Ellis, M. van Faassen, L. Fan, T.H. Fischer, C. Fonseca Guerra, S.J.A. van Gisbergen, A.W. Götz, J.A. Groeneveld, O.V. Gritsenko, M. Grüning, F.E. Harris, P. van den Hoek, C.R. Jacob, H. Jacobsen, L. Jensen, G. van Kessel, F. Kootstra, M.V. Krykunov, E. van Lenthe, D.A. McCormack, A. Michalak, J. Neugebauer, V.P. Nicu, V.P. Osinga, S. Patchkovskii, P.H.T. Philipsen, D. Post, C.C. Pye, W. Ravenek, J.I. Rodríguez, P. Ros, P.R.T. Schipper, G. Schreckenbach, J.G. Snijders, M. Solà, M. Swart, D. Swerhone, G. te Velde, P. Vernooijs, L. Versluis, L. Visscher, O. Visser, F. Wang, T.A. Wesolowski, E.M. van Wezenbeek, G. Wiesenekker, S.K. Wolff, T.K. Woo, A.L. Yakovlev, and T. Ziegler, Editon edn.
15. J. P. Perdew and B. edited by P. Ziesche and H. Eschrig (Akademie Verlag, in *91 Electronic Structure of Solids* Editon edn., 1991, p. 11.
16. J. P. Perdew, J. A. Chevary, S. H. Vosko, K. A. Jackson, M. R. Pederson, D. J. Singh and C. Fiolhais, *Physical Review B*, 1992, **46**, 6671-6687.
17. J. P. Perdew, J. A. Chevary, S. H. Vosko, K. A. Jackson, M. R. Pederson, D. J. Singh and C. Fiolhais, *Physical Review B*, 1993, **48**, 4978-4978.
18. D. Ballivet-Tkatchenko, H. Chermette, L. Plasseraud and O. Walter, *Dalton Transactions*, 2006, 5167-5175.
19. M. Poor Kalhor, H. Chermette, S. Chambrey and D. Ballivet-Tkatchenko, *Physical Chemistry Chemical Physics*, 2011, **13**, 2401-2408.
20. M. Poor Kalhor, H. Chermette and D. Ballivet-Tkatchenko, *Polyhedron*, 2012, **32**, 73-77.
21. L. Y. Ustynyuk, Y. A. Ustynyuk, D. N. Laikov and V. V. Lunin, *Russian Chemical Bulletin*, 2001, **50**, 376-380.

22. L. Y. Ustynyuk, Y. A. Ustynyuk, D. N. Laikov and V. V. Lunin, *Russian Chemical Bulletin*, 2001, **50**, 2050-2053.

23. Y. A. Ustynyuk, L. Y. Ustynyuk, D. N. Laikov and V. V. Lunin, *Journal of Organometallic Chemistry*, 2000, **597**, 182-189.

24. P. Hrobarik, V. Hrobarikova, A. H. Greif and M. Kaupp, *Angewandte Chemie-International Edition*, **51**, 10884-10888.

25. X. Solans-Monfort, J. S. Filhol, C. Coperet and O. Eisenstein, *New Journal of Chemistry*, 2006, **30**, 842-850.

# Figure captions

**Figure 1 :** Optimized geometries of **1-H** and **2-H.**

**Figure 2 :** Energy profile of the reaction between **1-H** and $N_2O$. Relevant distances (Å) and charges are given in Figures S1 and S2, respectively.

**Figure 1:** Changes in energy (eV) and shape of HOMOs and LUMOs of $N_2O$ and **1-H** via **TS1** (ΔE between HOMOs and LUMOs in italic).

**Figure 4:** Energy profile of the reaction between **2-H** and $N_2O$. Relevant distances (Å) and charges are given in Figures S4 and S5, respectively..

**Figure 5 :** Energy profile of the reaction between **1-H** and $CO_2$. Relevant distances (Å) and charges are given in Figures S8 and S9, respectively.

**Figure 6:** a) Energy profile of the reaction between **2-H** and first $CO_2$. Relevant distances (Å) and charges are given in Figures S7 and S8, respectively. b) Energy profile of the reaction between 2-(H)($\eta^2$-$O_2CH$) and second $CO_2$. Relevant distances (Å) are given in Figures S14**.**

Fig.1

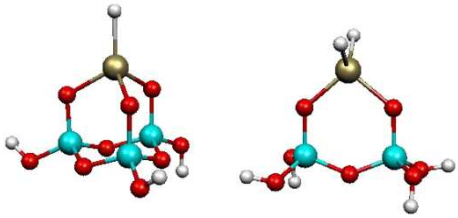

1-H 2-H

Fig.2

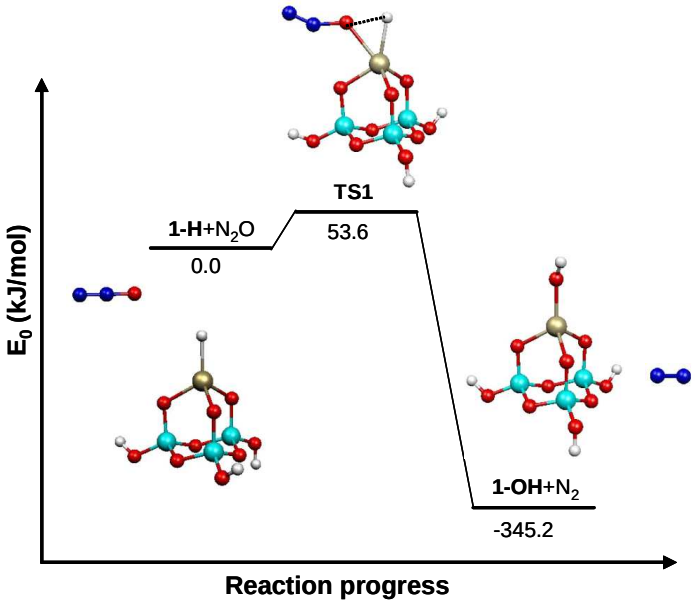

Fig.3

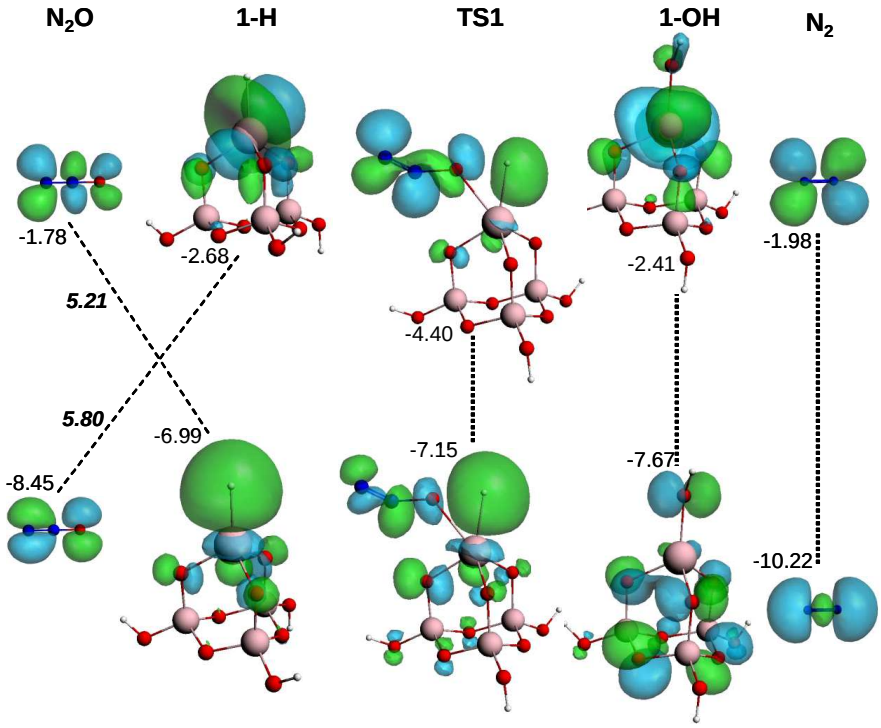

Fig.4

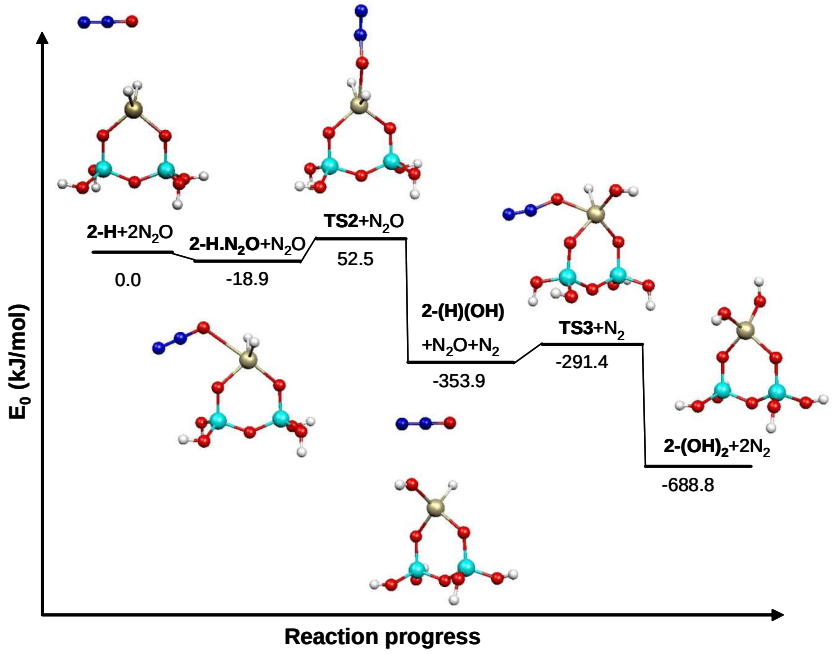

Fig.5

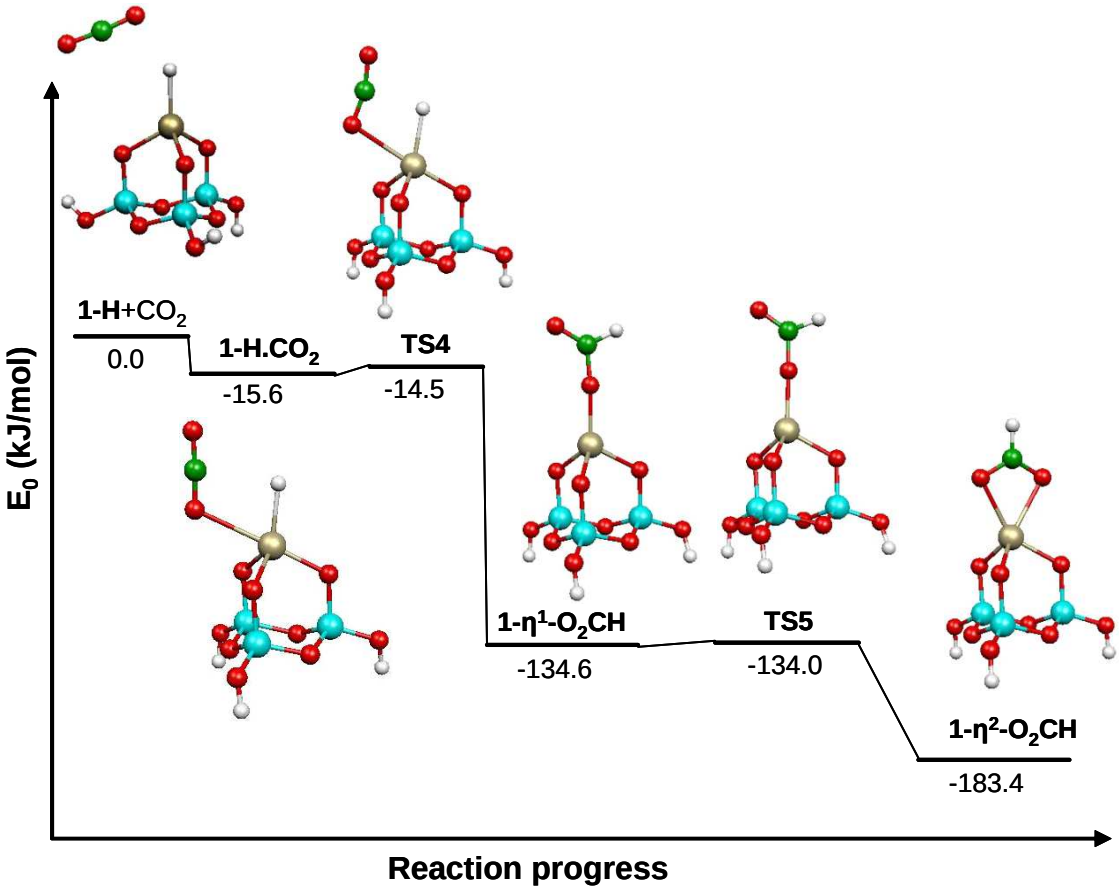

Fig. 6a

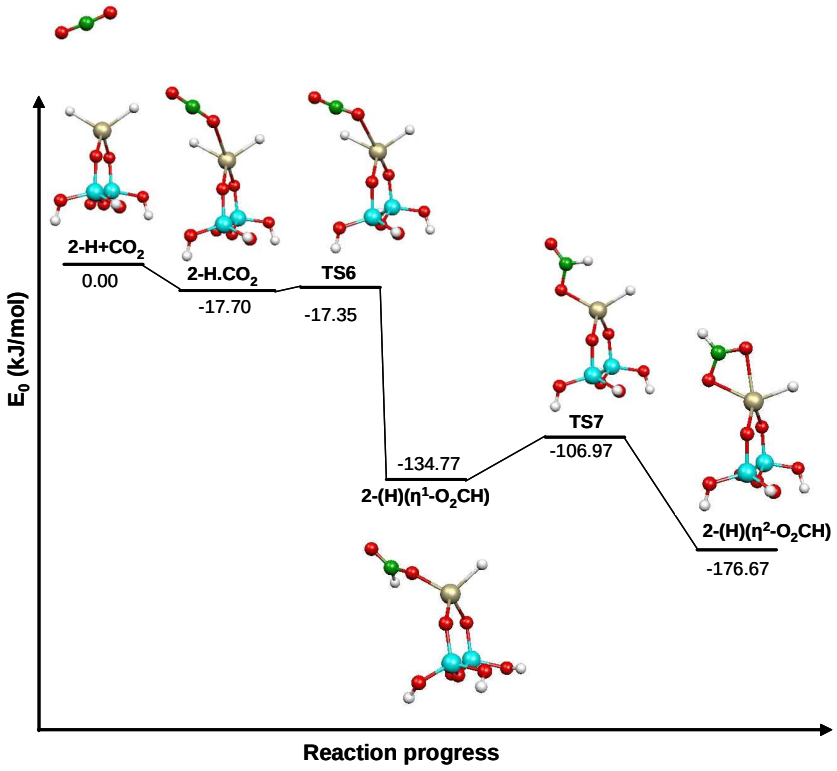

Fig.6b